Pergamon

Scripta Metallurgica et Materialia, Vol. 32, No. 7, pp. 1085–1089, 1995

0956-716X/95 $9.50 + .00

0956-716X(94)00008-5

ENVIRONMENTAL EFFECTS ON FIBER DEBONDING AND SLIDING IN AN SCS-6 SiC FIBER REINFORCED REACTION-BONDED Si_3N_4 COMPOSITE

J.I. Eldridge

NASA Lewis Research Center
Cleveland, OH 44135

(Received October 12, 1994)
(Revised November 8, 1994)

Introduction

Because fiber/matrix interfacial mechanical properties are critical to the overall strength and toughness of fiber-reinforced composites, several test methods have been developed to evaluate fiber debonding and sliding behavior (1,2). Most interface testing of metal or ceramic matrix composites has been performed in room (laboratory) air at room temperature without considering the effects of moisture or testing environment on the test results. Even though chemical reactivity at the fiber/matrix interface may be insignificant at room temperature for these composites, it is well known that friction and wear between sliding surfaces can be strongly dependent on environment, even at room temperature (3,4). Therefore, awareness of the environmental sensitivity of interface testing is necessary for the reliable interpretation and comparison of interfacial mechanical property tests. In addition, such awareness is needed to prevent the potentially inaccurate prediction of the performance of composites intended for service in high altitude or space environments based on interface tests completed in laboratory ambient.

This paper will demonstrate the effect of environment on fiber debonding and sliding as evaluated by fiber push-out testing at room temperature of an SCS-6 SiC fiber reinforced reaction-bonded Si_4N_4 matrix composite (SCS-6/RBSN). SCS-6/RBSN is a promising candidate material for component applications in advanced heat engines, and its low fiber/matrix interfacial shear strength is a key determinant in its demonstrated toughness (as evidenced by graceful failure beyond matrix cracking).

Experimental Procedure

Fabrication of the unidirectional SCS-6/RBSN composites is reported elsewhere (5). For fiber push-out testing, samples were sliced perpendicular to the fiber axis with a diamond saw and mechanically polished down to a 1 μm finish on both faces. The final thickness for all test specimens was 1.18 mm. Specimens

were then tested in a fiber push-out apparatus developed for elevated temperature testing (6). The fiber push-out tests were performed inside a cubical chamber where the environment could be controlled. A 112 μm diameter tungsten carbide punch was used to push out the 142 μm diameter SCS-6 fibers which were aligned over 300 μm diameter grooves in the specimen support block. Tests were performed at room temperature (28 to 32°C) in static room air (25-30% relative humidity), flowing dry air (3 ppm H_2O max.), flowing nitrogen (99.9995% pure), and vacuum (low 10-6 torr range). Eight to ten fibers were tested for each environment. Load versus time data were collected by computer, and the time data were converted to shaft displacement (equivalent to crosshead displacement of an Instron-type loading frame) using the indenter/shaft speed of 1.06 μm/s.

Results

Fig. 1 shows a typical load versus displacement plot indicating the features corresponding to different stages of fiber debonding and sliding. The peak load preceding a sharp load decrease was identified as the debonding load, P_d, which is the load at which the fiber is completely debonded. After debonding, the load is supported solely by frictional resistance to fiber sliding. Because there is not always a singular feature associated with friction during fiber sliding, two points were selected from each plot to represent the sliding behavior: $P_{\text{initial friction}}$ and $P_{\text{advanced friction}}$ were assigned to be the measured loads occurring at 2 and 20 μm of shaft/indenter motion beyond the debonding load, respectively. Note that because of system compliance the shaft/indenter displacements do not translate exactly to fiber displacements.

Fig. 2 shows representative push-out curves for the four environments tested. Fig. 3 summarizes all the tests by displaying the mean values along with the upper half of the 95% confidence interval for the mean for P_{debond}, $P_{\text{initial friction}}$, and $P_{\text{advanced friction}}$ for all four environments. The right-hand scale of Fig. 3 converts the load to average shear stress by the simple relation $\tau = P/\pi d_f t$, where τ is the average shear stress, d_f is the fiber diameter, and t is the specimen thickness.

Discussion

Both Figs. 2 and 3 indicate that while the testing environment had little effect on the fiber debonding load, substantial differences were observed for the frictional sliding loads. In contrast to the low, stable frictional sliding loads measured in room air, tests in vacuum and nitrogen showed dramatically increasing frictional sliding loads, while tests in dry air showed modestly increasing frictional sliding loads with continued fiber displacement. The disparities in fiber sliding loads increased with continued fiber sliding (contrast was greater for $P_{\text{advanced friction}}$ than for $P_{\text{initial friction}}$).

Increasing frictional sliding loads with continued fiber sliding suggests the occurrence of wear (6). Build-up of wear debris between the sliding fiber and matrix would tend to make fiber sliding increasingly difficult. The sensitivity of the degree of wear to the environment can be attributed to the well-documented (7,8) dependence on adsorbed species for the lubricative properties of graphite. The low friction and wear of graphite surfaces in air has been shown to depend primarily on water and, secondarily, on oxygen adsorption (7). In the absence of adsorbed species, sliding graphite surfaces exhibit dusting wear, producing extremely fine debris (7,8). The SCS-6 coating is not a crystalline graphite, but rather a complex turbostratic carbon coating with graded distributions of SiC particles embedded within the coating (9). Despite this complicated structure, Eldridge and Honecy (10) have shown that the two observed locations for interfacial failure in SCS-6/RBSN (within the coating structure and between the coating and the fiber) are in regions depleted of SiC particles. Therefore, it would be expected that sliding surfaces in these mostly turbostratic carbon regions would exhibit friction and wear behavior similar to graphite. Once the SCS-6 fiber debonds and moves, the gap produced at the failed interface will expose both sides of the interface to the ambient environment, and the sliding surfaces will exhibit environmental sensitivity of friction and wear similar to that of graphite.

The relatively low frictional sliding loads measured in dry air compared to nitrogen or vacuum indicate

oxygen has a significant effect in suppressing wear at the sliding surfaces. However, the frictional sliding loads measured in dry air were not as low as those measured in room air, indicating that oxygen alone was not as effective as a combination of oxygen and moisture in maintaining low friction. Because the effects of oxygen and moisture are not expected to be additive, it is not possible from these results to determine which plays the greater role in maintaining low friction and wear in room air.

Conclusions

There is a clear effect of testing environment on the frictional sliding behavior of fibers during push-out tests for SCS-6/RBSN. The evidence suggests that the presence of moisture and/or oxygen contribute to maintaining low levels of friction and wear during fiber sliding, where the sliding surfaces are exposed to the ambient environment. There-fore, awareness of possible environmental effects is necessary for reliable interpretation of any test of fiber/matrix interfacial mechanical properties. In addition, this environmental sensitivity has important implications for the performance of composites in different environments. For example, based on the results presented here, it is expected that crack-bridging fibers in SCS-6/RBSN would offer much more resistance to matrix crack opening in vacuum or inert environments than in air.

Acknowledgments

The author wishes to thank R.T. Bhatt for providing the composite specimens, and T. Spalvins, H.E. Sliney, and D.R. Wheeler for helpful discussions.

References

1. A.G. Evans and F.W. Zok, J. Mater. Sci. 29, 3857 (1994).
2. R.J. Kerans, R.S. Hay, N.J. Pagano, and T.A. Parthasarathy, Ceram. Bull. 68, 429 (1989).
3. J.K. Lancaster, Tribol. Int. 23, 371 (1990).
4. H.E. Sliney, Solid Lubricants, in Metals Handbook, vol. 18, p. 113, ASM International, Materials Park, OH (1993).
5. R.T. Bhatt, Mechanical Properties of SiC Fiber-Reinforced Reaction-Bonded Si_3N_4 Composites, NASA TM-87085 (1985).
6. J.I. Eldridge and B.T. Ebihara, J. Mater. Res. 9, 1035 (1994).
7. R.H. Savage, J. Appl. Phys. 19, 1 (1948).
8. J.K. Lancaster and J.R. Pritchard, J. Phys. D: Appl. Phys. 14, 747 (1981).
9. X.J. Ning and P. Pirouz, J. Mater. Res. 6, 2234 (1991).
10. J.I. Eldridge and F.S. Honecy, J. Vac. Sci. Technol. A 8, 2101 (1990).

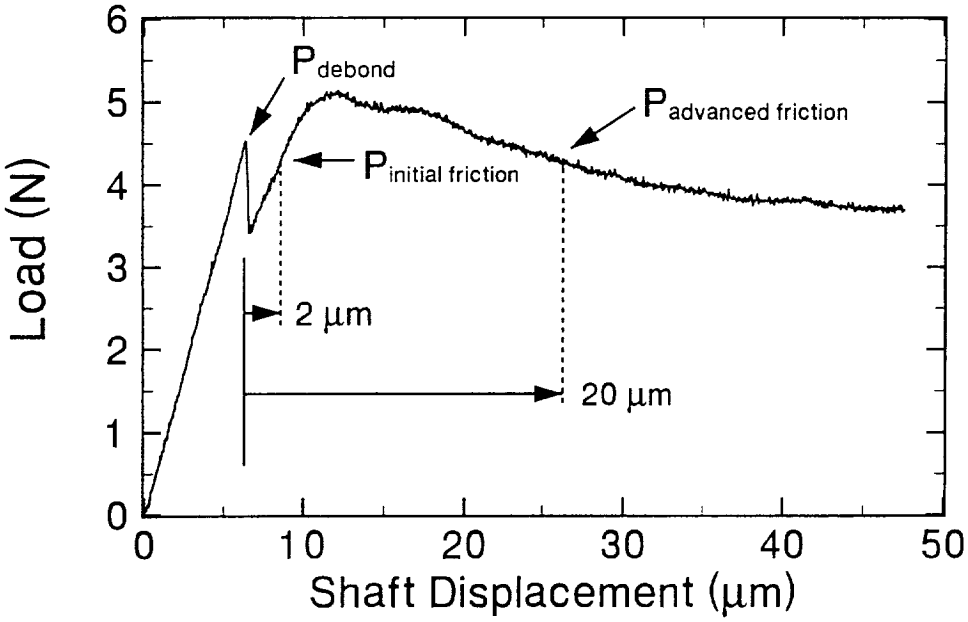

Fig. 1. Typical room-temperature fiber push-out load/displacement plot for 1.18 mm thick SCS-6/RBSN specimen in room air. Loads associated with complete debonding (P_d), initial friction ($P_{\text{initial friction}}$), and advanced friction ($P_{\text{advanced friction}}$) are identified.

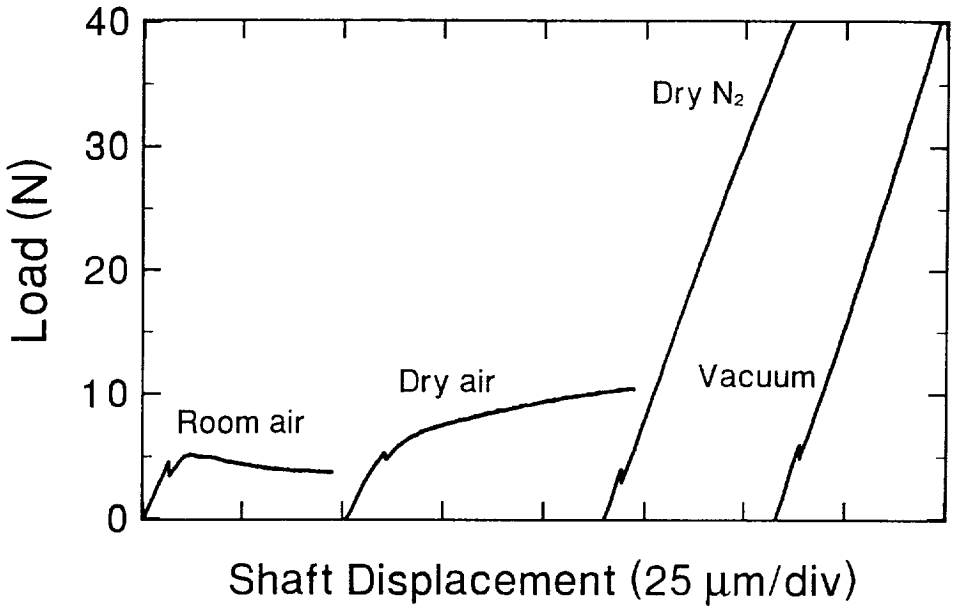

Fig. 2. Representative room-temperature fiber push-out load/displacement plots for 1.18 mm thick SCS-6/RBSN specimens tested in different environments. Plots have been offset along horizontal axis for easier comparison.

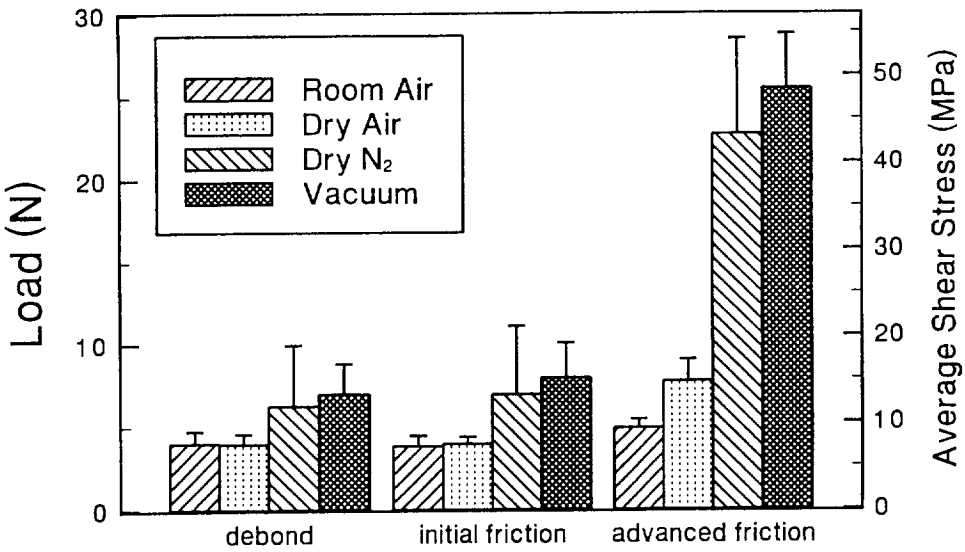

Fig. 3. Mean values (and upper halves of 95% confidence intervals) for debonding, initial frictional, and advanced frictional sliding loads from room-temperature fiber push-out tests of 1.18 mm thick SCS-6/RBSN specimens in different environments. Right-hand scale shows average shear stress corresponding to applied loads.